Published in final edited form as:
Cell. 2009 October 16; 139(2): 285–298. doi:10.1016/j.cell.2009.07.047.

Norrin, Frizzled4, and Lrp5 signaling in endothelial cells controls a genetic program for retinal vascularization

Xin Ye[1,7], **Yanshu Wang**[1,4,7], **Hugh Cahill**[2], **Minzhong Yu**[5], **Tudor C. Badea**[1,4], **Philip M. Smallwood**[1,4], **Neal S. Peachey**[5,6], and **Jeremy Nathans**[1,2,3,4]

[1] Department of Molecular Biology and Genetics, Johns Hopkins University School of Medicine, Baltimore, Maryland 21205

[2] Department of Neuroscience, Johns Hopkins University School of Medicine, Baltimore, Maryland 21205

[3] Department of Ophthalmology, Johns Hopkins University School of Medicine, Baltimore, Maryland 21205

[4] Howard Hughes Medical Institute, Johns Hopkins University School of Medicine, Baltimore, Maryland 21205

[5] Cole Eye Institute, Cleveland Clinic Foundation, Cleveland, Ohio 44195

[6] Research Service, Cleveland VA Medical Center, Cleveland, Ohio 44106

SUMMARY

Disorders of vascular structure and function play a central role in a wide variety of CNS diseases. Mutations in the Frizzled4 (Fz4) receptor, Lrp5 co-receptor, or Norrin ligand cause retinal hypovascularization, but the role of Norrin/Fz4/Lrp signaling in vascular development has not been defined. Using mouse genetic and cell culture models, we show that loss of Fz4 signaling in endothelial cells causes defective vascular growth, which leads to chronic but reversible silencing of retinal neurons. Loss of Fz4 in all endothelial cells disrupts the blood brain barrier in the cerebellum, while excessive Fz4 signaling disrupts embryonic angiogenesis. Sox17, a transcription factor that is up-regulated by Norrin/Fz4/Lrp signaling, plays a central role in inducing the angiogenic program controlled by Norrin/Fz4/Lrp. These experiments establish a cellular basis for retinal hypovascularization diseases due to insufficient Frizzled signaling, and they suggest a broader role for Frizzled signaling in vascular growth, remodeling, maintenance, and disease.

Address for editorial correspondence: Dr. Jeremy Nathans, 805 PCTB, 725 North Wolfe Street, Johns Hopkins University School of Medicine, Baltimore, MD 21205, tel: 410-955-4679, FAX: 410-614-0827, jnathans@jhmi.edu.
[7] co-first authors

SUPPLEMENTAL DATA

Supplemental Data including Supplemental Experimental Procedures, seven figures and four tables can be found with this article at XXX.

Accession Numbers

Microarray hybridization data have been deposited in the GEO database with accession code GSE16841.

INTRODUCTION

The mature vasculature can be divided into arteries, veins, and capillaries, and vascular cells into endothelial cells (ECs) and mural cells (MCs), with additional anatomic, cellular, and molecular diversity in each of these categories. The vasculature is generated by precisely orchestrated patterns of vasculogenesis and/or angiogenesis followed by remodeling and stabilization concurrent with the establishment of endothelial cell (EC)–mural cell (MC) interactions (Armulik et al., 2005). In keeping with the complexity of vascular development and structure, multiple cell signaling systems – including the VEGF, Netrin, Ephrin, Notch, and Angiopeitin systems – have been implicated in coordinating the proliferation, migration, adhesion, and differentiation of vascular cells (Adams and Alitalo, 2007).

The present study focuses on the retinal vasculature. This vasculature plays a central role in a variety of ocular diseases, including diabetic retinopathy and retinopathy of prematurity (Gariano and Gardner, 2005). The retinal vasculature presents a simple and stereotyped architecture. The major arteries and veins reside on the vitreal face of the retina and are oriented radially from their origin at the optic disc. They give rise to a series of smaller vessels that penetrate the retina and connect to a pair of planar capillary beds flanking a central layer of neurons (the inner nuclear layer). In the mouse, as in other mammals, the initial phase of retinal vascular development is characterized by radial growth from the optic disc, followed by the development of the intra-retinal capillaries.

An unusual signaling system with profound effects on retinal vascular development has emerged from the study of Norrie disease, familial exudative vitreoretinopathy (FEVR), and osteoporosis-pseudoglioma syndrome (Berger and Ropers, 2001; Robataille et al., 2002; Jiao et al., 2004; Toomes et al., 2004; Ai et al., 2005). In these genetic diseases, retinal hypovascularization is caused by partial or complete loss-of-function mutations in the genes coding for the cystine knot protein Norrin, the integral membrane receptor Frizzled4 (Fz4), or the Fz4 co-receptor Lrp5, respectively. The similar retinal hypovascularization phenotypes observed in *Ndp* (*Norrie disease protein*), *Fz4*, or *Lrp5* loss-of-function mouse models, the high affinity and specificity of Norrin-Fz4 binding, and the potent activation of canonical Wnt signaling following co-expression of Norrin, Fz4, and Lrp5 imply that Norrin is an in vivo ligand for Fz4 (Kato et al, 2002; Xu et al., 2004; Richter et al., 1998; Luhmann et al., 2005b; Smallwood et al., 2007; Xia et al., 2008).

These observations raise a series of inter-related questions that are central to understanding the cellular basis and functional significance of Norrin/Fz4/Lrp signaling. Is the primary site of Fz4 signaling - and hence the primary cellular defect in inherited diseases in which this system is impaired - neuronal, glial, or vascular? At the physiological and behavioral levels, what aspects of visual function are impaired by vascular defects that result from loss of Fz4 signaling? What cellular processes in vascular development require Fz4 signaling in the intact animal and in cell culture? Is Fz4 signaling a general feature of vascular development outside of the retina? Does Fz4 signaling alter gene expression, and, if so, how does this relate to vascular development? In the present work, we have addressed these questions by studying the effects of gain and/or loss of Fz4 signaling in vivo and in cell culture.

RESULTS

An essential role for *Fz4* in retinal ECs

To assess the pattern of *Fz4* expression and to permit cell type-specific deletion of *Fz4* while simultaneously marking cells, we generated the *Fz4* conditional knockout (CKO) allele $Fz4^{CKOAP}$ (Figure 1A). In the absence of Cre-mediated recombination, $Fz4^{CKOAP}$ functions as a wild-type (WT) allele and the distal alkaline phosphatase (AP) is not expressed. *Cre-*

mediated recombination excises the *Fz4* coding and 3′ UTR and places AP under the control of the *Fz4* promoter. Thus, Cre-mediated recombination converts $Fz4^{CKOAP/+}$ cells into phenotypically WT $Fz4^{AP/+}$ cells. When $Fz4^{CKOAP}$ is in combination with a conventional *Fz4* knockout allele (Wang et al., 2001), Cre-mediated recombination converts phenotypically WT $Fz4^{CKOAP/-}$ cells into mutant $Fz4^{AP/-}$ cells.

In $Fz4^{CKOAP/+}$*;Sox2-Cre* mice, which produce Cre ubiquitously (Hayashi et al., 2002), the AP reporter is seen throughout the vasculature starting at embryonic day (E)8. Following Cre-mediated recombination in ECs [$Fz4^{CKOAP/+}$*;Tie2-Cre*; Figure 1B; Kisanuki et al., 2001)], or in MCs [$Fz4^{CKOAP/+}$*;PDGFRB-Cre* (Foo et al., 2006)], $Fz4^{AP}$ expression is maintained through adulthood (Figure S1).

In the retina, *Fz4* is expressed in ECs, MCs, photoreceptors, and a subset of inner retinal neurons (Figure S1C–E; Wang et al., 2001). To determine the cell type(s) responsible for the $Fz4^{-/-}$ retinal vascular phenotype, we deleted *Fz4* in ECs with *Tie2-Cre*, in MCs with *PDGFRB-Cre* (Cre-mediated recombination in this case is incomplete), and in most or all retinal neurons and glia with *Rx-Cre* (Swindell et al., 2006). In the latter two cases, there was little or no change in retinal vascular morphology (Figure S2), although, as described more fully below, the $Fz4^{AP/-}$ MCs in the $Fz4^{CKOAP/-}$*;PDGFRB-Cre* retina are abnormal. By contrast, in adult $Fz4^{CKOAP/-}$*;Tie2-Cre* mice, intraretinal capillaries are completely absent, vessels penetrating from the vitreal surface terminate in ball-like clusters, large vessels are dilated and form arterio-venous anastomoses, and intraocular hemorrhages are common (Figure 1C). These retinal vascular defects closely resemble those seen in $Fz4^{-/-}$, $Lrp5^{-/-}$, and Ndp^{-} mice (see Figure 3A below; Xu et al., 2004; Luhmann et al., 2005b; Xia et al., 2008), indicating that defective Fz4 signaling in retinal ECs (RECs) recapitulates these loss-of-function phenotypes.

To determine whether Fz4 acts in a cell autonomous manner, we took advantage of the observation that ~5% of $Fz4^{CKOAP/+}$*;Tie2-Cre* and $Fz4^{CKOAP/-}$*;Tie2-Cre* retinas exhibit incomplete Cre-mediated recombination (Figure 1D). In incompletely recombined $Fz4^{CKOAP/+}$*;Tie2-Cre* retinas, $Fz4^{AP/+}$ RECs populate relatively contiguous territories encompassing both large and small vessels within all three vascular layers. Each of these contiguous territories is presumably composed of the clonal progeny of one or more REC progenitors that underwent a Cre-mediated recombination event (Figure 1Da).

Several distinctive features characterize $Fz4^{AP/-}$ RECs in $Fz4^{CKOAP/-}$*;Tie2-Cre* retinas with incomplete recombination (Figure 1D, b–d). First, there was a strong predilection for $Fz4^{AP/-}$ RECs to remain confined to vessels at the vitreal surface, implicating Fz4 signaling specifically in the development of intra-retinal capillaries. Second, in contiguous territories populated by $Fz4^{AP/-}$ RECs, ball-like clusters of RECs characteristic of the $Fz4^{-/-}$ vasculature were seen instead of intraretinal capillaries. Third, at the boundaries of large clones of $Fz4^{AP/-}$ RECs, some $Fz4^{AP/-}$ RECs were integrated into the adjacent WT capillary network, suggesting that close proximity between WT and $Fz4^{AP/-}$ RECs can partially correct the defects associated with loss of *Fz4*. Fourth, in regions of retina populated by non-recombined (i.e. AP-negative) RECs, rare $Fz4^{AP/-}$ RECs were observed in all classes of blood vessels, including intraretinal capillaries. These $Fz4^{AP/-}$ RECs likely arose from Cre-mediated recombination among $Fz4^{CKOAP/-}$ RECs that were already part of a capillary network, implying that *Fz4* is not absolutely or immediately required to maintain the capillary REC phenotype once that phenotype has been established.

Muller glia are the principle source of Norrin

To localize the site(s) of *Ndp* expression, we inserted an AP reporter into exon 2 in the *Ndp* 5′ UTR (Figure 1E). *Ndp* is X-linked, and histochemical staining for AP in Ndp^{AP} males showed homogeneous AP staining throughout the retina at P4, P7, and in adulthood. To visualize

individual cell morphologies, we took advantage of the tissue mosaicism generated by X-chromosome inactivation in $Ndp^{AP/+}$ females. At P4, P7, and adulthood, AP activity was localized to vertical stripes spanning the full thickness of the retina, indicative of expression in Muller glia (Figure 1F). Flat mounts of $Ndp^{AP/+}$ female retinas at P7 show no detectable AP expression in retinal ganglion cells (RGCs) or astrocytes (Figure 1F). Thus, Muller glia produce Norrin, which then activates Fz4 on RECs.

Defects in visual function in *Fz4*$^{-/-}$ mice caused by retinal vascular insufficiency

Vision loss is a hallmark of FEVR, but it is not known whether this is entirely due to vascular insufficiency or whether there are contributions from the loss of Fz4 signaling in neurons. To characterize the type, severity, and anatomic origin of visual deficits associated with loss of Norrin/Fz4/Lrp signaling, we measured rod- and cone-mediated full-field electroretinographic (ERG) responses in $Fz4^{-/-}$, $Fz4^{CKOAP/-}$*;Rx-Cre*, and $Fz4^{CKOAP/-}$*;Tie2-Cre* mice and in control WT, $Fz4^{CKOAP/+}$*;Rx-Cre*, and $Fz4^{CKOAP/+}$*;Tie2-Cre* mice (Figure 2A–C), and then analyzed each retina by whole-mount AP histochemistry. Photoreceptor (a-wave) and inner retinal (b-wave) ERG responses in the pan-neuronal/panglial *Fz4* knockout retina ($Fz4^{CKOAP/-}$*;Rx-Cre*) were indistinguishable from WT. By contrast, in $Fz4^{-/-}$ and $Fz4^{CKOAP/-}$*;Tie2-Cre* mice, while the a-wave was unaffected, the b-wave was markedly reduced, indicating a defect in the inner retinal ON pathway (McCall and Gregg, 2008). This ERG phenotype matches that reported previously for Ndp^{-} mice (Luhmann et al., 2005b). Despite the expression of *Fz4* in photoreceptors and other retinal neurons, these observations indicate that the ERG defect is caused by the absence of Norrin/Fz4/Lrp signaling in the vasculature rather than in neurons or glia.

To assess the behavioral consequences of retinal vascular dysfunction, we tested the optokinetic reflex (OKR) and the pupillary light response. OKR testing showed that, in the absence of *Fz4*, rod and cone signals are not transmitted effectively, and this block arises from a primary defect in the vasculature (Figure 2D,E). Interestingly, the OKR defect in $Fz4^{-/-}$ and $Fz4^{CKOAP/-}$*;Tie2-Cre* mice is more severe than the OKR defect associated with genetic silencing of the ON pathway in $mGluR6^{-/-}$ mice (Iwakabe et al., 1997), consistent with a model in which the OKR is driven by both the ON and OFF pathways and indicating that both pathways are compromised in $Fz4^{-/-}$ and $Fz4^{CKOAP/-}$;Tie2-Cre mice.

In contrast to the OKR, light-dependent pupil constriction is minimally impaired by the loss of *Fz4* (Figure 2F), indicating that the melanopsin-expressing intrinsically photosensitive RGC, which control pupil constriction (Hattar et al., 2003), remain active in the $Fz4^{-/-}$ retina. These data are consistent with earlier studies showing an absent OKR and near normal pupil response in mice that are missing both rod and cone function (Hattar et al., 2003; Cahill and Nathans, 2008).

Despite a chronic vascular insufficiency that precludes normal responses of horizontal, bipolar, and/or amacrine cells in Ndp^{-}, $Fz4^{-/-}$ and $Fz4^{CKOAP/-}$*;Tie2-Cre* retinas, the mutant retinas appear surprisingly normal (Figure 3A and S3). This observation suggested that it might be possible to revive these neurons to the point where they could transmit photoreceptor signals. To test this idea, we recorded light responses from the ganglion cell layer in WT and $Fz4^{-/-}$ retinas ex vivo using a multi-electrode array (Meister et al., 1994). In this preparation, oxygen, glucose, and other small molecules passively diffuse into the retina, obviating any need for the vasculature. As seen in Figure 2G, ganglion cell layer neurons in the adult $Fz4^{-/-}$ retina exhibit ON, OFF, and ON-OFF action potential responses to local changes in illumination. The number of ON, OFF, and ON-OFF subtypes identified in the retinas of $Fz4^{-/-}$ mice were 4, 55, and 12, respectively; the number of ON, OFF, and ON-OFF subtypes identified in the retinas of WT littermates were 19, 21, and 16, respectively. In sum, the ERG, OKR, pupil constriction, and multi-electrode array experiments reported here indicate that a chronic absence of intra-

retinal capillaries leads to a severe and localized - but still largely reversible - block to neurotransmission through the inner nuclear layer.

Norrin/Fz4/Lrp signaling controls vascular growth and EC-MC interactions

To assess the relative contributions of Norrin, Fz4, and Lrp5 to retinal vascular growth and patterning, we compared WT, *Fz4*$^{-/-}$, *Fz4*$^{CKOAP/-}$*;Tie2-Cre*, *Lrp5*$^{-/-}$, and *Ndp*$^{-}$ (Figure S4) mice with respect to (1) the appearance of the vasculature in the adult (Figure 3A), (2) vascular growth during the first postnatal week (Figure 3B and C), and (3) vascular density at P7 (Figure 3D). Although the initial vascular invasion of the retina was unaffected by any of the mutations, *Fz4*$^{-/-}$, *Fz4*$^{CKOAP/-}$*;Tie2-Cre*, and *Ndp*$^{-}$ retinas exhibited retarded vascular growth and sparse vascular coverage, as reported previously in *Fz4*$^{-/-}$ and *Ndp*$^{-}$ retinas (Xu et al., 2004; Luhmann et al., 2005b). By each of these measures, *Lrp5*$^{-/-}$ retinas show a more modest phenotype. These observations suggest that Norrin is the only Fz4 ligand relevant to retinal angiogenesis, and that there may be a partial contribution to co-receptor function from Lrp6, a close homologue of Lrp5.

MCs are required both to stabilize the nascent vasculature and to maintain the permeability barrier of the mature vasculature, and, in particular, the blood brain barrier (BBB) and the blood retina barrier (BRB) (Armulik et al., 2005; Zlokovic, 2008). The sparse vasculature in *Fz4*$^{-/-}$ and *Ndp*$^{-}$ retinas (Figure 3B and D), the defective cerebellar BBB associated with loss of *Fz4* (see Figure 4A below), and the defective BRB associated with loss of *Ndp* or *Fz4* (Xu et al., 2004; Luhmann et al., 2005b) suggested that Norrin/Fz4/Lrp signaling might control EC-MC interactions. This hypothesis is consistent with the expression of *Fz4* in both ECs and MCs, and, as described below, it is strongly supported by the defective EC-MC interactions in the absence of Norrin/Fz4/Lrp signaling.

At P2, at the start of REC outgrowth, EC-MC interactions are already strikingly aberrant in *Fz4*$^{-/-}$ retinas, indicating an initial failure of EC-MC recognition or adhesion (Figure 3E). At P7, in both *Fz4*$^{-/-}$ and *Ndp*$^{-}$ retinas, MCs are thinner and MC density is lower than in WT retinas, resulting in incomplete coverage of veins and capillaries (Figure 3F). In contrast, arterial coverage by vascular smooth muscle cells (vSMCs) is minimally affected in *Fz4*$^{-/-}$ and *Norrin*$^{-}$ retinas. Quantification of MC coverage of the radial veins at P7 shows a defect in *Fz4*$^{CKOAP/-}$*;Tie2-Cre* retinas that is almost as severe as that found in *Fz4*$^{-/-}$ and *Ndp*$^{-}$ retinas; a milder defect is found in *Lrp5*$^{-/-}$ retinas (Figure 3G). Interestingly, between P7 and P9, MC coverage of veins in *Fz4*$^{CKOAP/-}$*;Tie2-Cre* retinas increased significantly ($p<0.0001$, student t-test), and by P9 it was higher than that in *Fz4*$^{-/-}$ or *Norrin*$^{-}$ retinas ($p<0.0001$, ANOVA).

The difference in the severity of MC coverage defects between *Fz4*$^{CKOAP/-}$*;Tie2-Cre* and *Fz4*$^{-/-}$ retinas (Figure 3G) indicates that EC-MC interactions depend on *Fz4* function in at least one cell type in addition to ECs. To test the obvious possibility that the additional cell type is the MC, we visualized *Fz4*$^{AP/+}$ MCs in *Fz4*$^{CKOAP/+}$*;PDGFRB-Cre* retinas and *Fz4*$^{AP/-}$ MCs in *Fz4*$^{CKOAP/-}$*;PDGFRB-Cre* retinas (Figure 3H). While *Fz4*$^{AP/+}$ MCs efficiently cover both arteries and veins, *Fz4*$^{AP/-}$ MCs provide substantially lower coverage of veins: in control *Fz4*$^{CKOAP/+}$*;PDGFRB-Cre* retinas at P30, 65% of veins and 63% of arteries show >90% coverage by AP-expressing MCs; whereas in *Fz4*$^{CKOAP/-}$*;PDGFRB-Cre* retinas at P30, 55% of arteries and only 8% of veins show >90% coverage. These results demonstrate an essential role for Norrin/Fz4/Lrp signaling in ECs to promote vascular growth, and in both ECs and MCs to promote their mutual interaction.

Fz4 is required for vascular integrity in the cerebellum

In addition to retinal vascular defects, *Fz4*$^{-/-}$ mice exhibit a progressive cerebellar degeneration (Wang et al., 2001). Although *Ndp*$^{-}$ mice do not exhibit this phenotype, both *Fz4*$^{-/-}$ and

Ndp^{-} mice show a progressive reduction in vascular density in the cerebellum, suggesting a defect in vascular integrity and/or stability (Xu et al., 2004; Luhmann et al., 2008). Consistent with this hypothesis, we commonly observe hemorrhages in the cerebellum but not in the cerebral cortex in *Fz4*$^{-/-}$ brains.

To test the role of Fz4 signaling in the cerebellar vasculature, we monitored the BBB by immunostaining for mouse IgG in freshly frozen sections of *Fz4*$^{CKOAP/-}$*;Tie2-Cre*, control *Fz4*$^{CKOAP/+}$*;Tie2-Cre*, and *Ndp*$^{-}$ brains. In the absence of an intact BBB, IgG can pass from the intravascular space into the surrounding tissues. As seen in Figure 4A, in brain sections that include both cerebellum and cortex, only the *Fz4*$^{CKOAP/-}$*;Tie2-Cre* cerebellum showed a defect in BBB integrity. An identical vascular phenotype was seen in *Fz4*$^{-/-}$ brains (data not shown), and transmission electron microscopy of WT and *Fz4*$^{-/-}$ cerebella shows, in the latter, misshapen capillaries and protrusions of endothelial processes into the vessel lumen (Figure S5). Importantly, quantification of granule cell apoptosis in WT, *Fz4*$^{CKOAP/-}$*;Tie2-Cre*, and *Fz4*$^{-/-}$ cerebella at P18 demonstrate that the *Fz4*$^{-/-}$ cerebellar degeneration is of vascular origin (Figure 4B,C).

These experiments indicate a major role for Fz4 signaling in maintaining the integrity of the cerebellar vasculature, presumably in response to Norrin and/or Wnt binding. Consistent with this conclusion, recent evidence indicates that Wnt7a and Wnt7b expressed in the developing CNS promote CNS-type vascular development, including BBB development (Stenman et al., 2008; Daneman et al., 2009).

Over-activation of Fz4/Lrp signaling disrupts embryonic angiogenesis

A growing number of observations imply that Norrin/Fz4 or Wnt/Fz4 signaling plays a role in vascular development or maintenance outside of the retina. First, *Fz4*$^{-/-}$ and *Ndp*$^{-}$ mice exhibit a progressive loss of blood vessels within the stria vascularis that is associated with hearing loss (Rehm et al., 2002; Xu et al., 2004); similarly, more than a third of Norrie disease patients experience hearing loss (Berger and Ropers, 2001). Second, in two families, *NDP* mutations have been associated with both Norrie disease and peripheral vascular insufficiency (Rehm et al., 1997; Michaelides et al., 2004). Third, female *Fz4*$^{-/-}$ and *Ndp*$^{-}$ mice exhibit defects in corpora lutea formation and endometrial vascularization of the placenta, respectively, processes that require rapid vascular growth and remodeling (Hsieh et al., 2005; Luhmann et al., 2005a). The observation of *Fz4*^{AP} expression throughout the developing and adult vasculature (Figures 1B and S1) is also consistent with a wider role for Fz4 signaling in vascular biology.

To explore this idea, we asked whether Fz4 signaling induced by ectopic Norrin could modify vascular development. To produce Norrin ectopically, we targeted a Cre-activated *Norrin* cassette to the *Ubiquitin-b* (*Ubb*) locus, the site of transgene insertion in the *Z/AP* mouse line (Figure 5A; Lobe et al., 1999; T. Rotolo and J.N., unpublished); we will refer to this knock-in allele as "*Z/Norrin*". In *Z/Norrin;Sox2-Cre* mice, Cre-mediated recombination occurs early in embryogenesis, producing a severe disruption in angiogenesis and midgestational lethality. Although most *Z/Norrin;Sox2-Cre* embryos are still alive at E10.5, they are growth retarded and have severely disorganized embryo and yolk sac vasculatures (Figure 5B,C). Moreover, at E9.5, when vSMCs begin to surround the dorsal aorta in WT embryos, the aorta in *Z/Norrin;Sox2-Cre* embryos has no associated vSMCs (Figure 5D).

The defects caused by Norrin overproduction are fully suppressed in a *Fz4*$^{-/-}$ background (Figure 5E). Interestingly, in a *Fz4*$^{+/-}$ background, the *Z/Norrin;Sox2-Cre* phenotype is partially suppressed, leading to a milder phenotype at E10.5 and occasional survivors at E18 (Figure 5F and I). These experiments indicate that, in the embryonic vasculature, Fz4 is the major receptor for Norrin, and Fz4 signaling can potently modulate angiogenesis. The *Fz4*

dosage sensitivity is consistent with the mild-to-moderate vascular insufficiency observed in humans with FEVR who are heterozygous for presumptive loss-of-function or hypomorphic mutations in *Fz4*; a more severe phenotype has been reported in one individual with homozygous mutation of *Fz4* (Robitaille et al., 2002; Toomes et al., 2004; Xu et al., 2004; Qin et al., 2005; Kondo et al., 2007).

Partial rescue of the Norrin over-production phenotype was also obtained in an $Lrp5^{-/-}$ background (Figure 5G,H). The failure of the $Lrp5^{-/-}$ background to fully rescue the Norrin over-production phenotype could reflect signaling via Lrp6, which is expressed in both vascular and non-vascular cells in the E10.5 embryo and yolk sac (Figure S6).

Defects in the production of capillary-like structures by $Fz4^{-/-}$ REC lines

In all of the experiments described above, Norrin/Fz4/Lrp signaling was studied in vivo. To reduce this system to its simplest components, we asked whether RECs in culture recapitulate any of the phenotypic differences between WT and mutant mouse lines. To isolate the requisite REC lines, we crossed $Fz4^{-}$, Ndp^{-}, and $Lrp5^{-}$ alleles into the "Immorto-mouse" line (Jat et al., 1991). To prepare REC lines, adult retinas were dissociated, and vascular fragments were immuno-affinity purified using an anti-PECAM mAb (Figure 6A; Matsubara et al., 2000; Su et al., 2003). REC lines – defined as VE-cadherin^{+}, PECAM^{+}, and NG2^{-} epithelial cells - were obtained from WT (4 lines), Ndp^{-} (7 lines), $Lrp5^{-/-}$ (3 lines), and $Fz4^{-/-}$ (6 lines) Immorto-mice (Figure 6A).

In a simple test of cell migration, WT, $Fz4^{-/-}$, and $Lrp5^{-/-}$ REC lines showed substantial motility over a 24-hour interval in response to scratch wounding of a confluent monolayer (Figure 6B). An assay that more closely resembles vascular development is the formation of capillary-like networks by RECs cultured on Matrigel. In this assay, 4/4 WT, 3/3 $Lrp5^{-/-}$, and 6/7 Ndp^{-} REC lines showed robust network formation, whereas 6/6 $Fz4^{-/-}$ REC lines showed virtually no changes by the end of the standard six hour incubation (Figure 6C). Interestingly, when WT and $Fz4^{-/-}$ RECs were plated together on Matrigel, many of the $Fz4^{-/-}$ RECs adopted a more differentiated morphology and were incorporated into the WT capillary-like network (Figure 6D and movie S1). This cooperative behavior is reminiscent of the in vivo integration of some $Fz4^{AP/-}$ RECs into normal-appearing capillaries when mutant and WT RECs are in close proximity (Figure 1D). These observations suggest that $Fz4^{-/-}$ RECs are competent to receive, but are unable to send, a cell adhesion or cell motility signal.

It is interesting that $Lrp5^{-/-}$ RECs show no apparent defect in the Matrigel assay. Given the intermediate phenotype exhibited by $Lrp5^{-/-}$ RECs in vivo (Figure 3A,C,D, and G), we interpret this finding to mean that residual Norrin/Fz4/Lrp signaling – perhaps via Lrp6, which is expressed in RECs at levels comparable to Lrp5 (Figure S6) – may be sufficient to support capillary-like network formation by $Lrp5^{-/-}$ RECs.

A transcriptional program controlled by Norrin/Fz4/Lrp signaling

To explore the underlying molecular effectors of the angiogenic response to Norrin/Fz4/Lrp signaling, we analyzed genome-wide changes in transcript abundance resulting from either increased or decreased signaling. To identify the primary response to increased Norrin/Fz4/Lrp signaling, we compared WT and *Z/Norrin;Sox2-Cre* yolk sacs at E8.5 (prior to the appearance of any obvious Norrin-induced vascular changes). The yolk sac was chosen because it is easily dissected and it consists only of epithelial and vascular cells. 66 transcripts exhibited a >2-fold change with a P-value <0.05, and many code for proteins involved in cell-cell signaling and ECM structure and/or remodeling (Figure 7 and Table S1). By E10.5, when vascular morphology in the *Z/Norrin;Sox2-Cre* yolk sac is highly aberrant (Figure 5B and C), the number of transcripts with a >2-fold change had increased to 400. Interestingly, the

transcript coding for Sox17 - an HMG box transcription factor that has been implicated in endothelial development in mice and zebrafish (Matsui et al., 2006;Sakamoto et al., 2007;Pendeville et al., 2008) – was among the several transcripts with the highest increases in abundance in response to Norrin over-expression (Figure 7A).

To validate these results, the abundance changes of a subset of transcripts were determined by blot hybridization (Figure 7A, right). Increases were observed for transcripts coding for Timp3, a matrix metalloproteinase (MMP) inhibitor, Flt1, which functions as a VEGF sink, and several procollagens and procollagen processing enzymes, while a decrease was observed for transcripts encoding plasminogen. Transcripts coding for Flk1, the major mediator of VEGF signaling, remained unchanged. Increased production of vascular basement membrane components and reduced MMP activity and VEGF signaling should block vascular remodeling.

To characterize the effect on the transcriptome of a decrement in Norrin/Fz4/Lrp signaling, micro-array hybridization was performed with RNA from acutely dissociated and anti-PECAM immunoaffinity-purified adult WT, *Fz4*$^{-/-}$, *Lrp5*$^{-/-}$, and *Ndp*$^{-}$ retinal vascular cells and from P16 WT and *Fz4*$^{-/-}$ cerebellar vascular cells (Figure S7 and Supplementary Table 2). Consistent with the high degree of similarity in their retinal vascular phenotypes, the alterations in *Fz4*$^{-/-}$, *Lrp5*$^{-/-}$, and *Ndp*$^{-}$ retinal vascular transcriptomes were highly correlated and showed numerous differences vs. WT (Figure S7).

The differing behaviors of WT and *Fz4*$^{-/-}$ RECs on Matrigel imply corresponding molecular differences. Indeed, micro-array hybridization shows substantial differences between WT and *Fz4*$^{-/-}$ RECs, which presumably reflect Fz4 signaling in WT but not *Fz4*$^{-/-}$ RECs, perhaps in response to Norrin and/or Wnts in the fetal bovine serum present in the culture medium (Figure 7B). To directly test the Norrin response of WT and *Fz4*$^{-/-}$ RECs in culture, we co-cultured these cells either with a human embryonic kidney 293 cell line that stably expresses Norrin or with control 293 cells, and then analyzed their transcripts by micro-array hybridization (Figure 7C and Supplementary Table 4). Earlier experiments with a reporter cell line had shown that co-culture with Norrin-secreting 293 cells is an effective way to activate Fz4/Lrp signaling (Xu et al., 2004). Figure 7C shows that WT and *Fz4*$^{-/-}$ RECs differ markedly in their response to co-culture with Norrin-expressing 293 cells. Consistent with the WT vs. *Z/Norrin;Sox2-Cre* yolk sac comparisons described above, *Sox17* transcripts are more abundant in WT RECs compared to *Fz4*$^{-/-}$ RECs, and are induced by Norrin in WT but not in *Fz4*$^{-/-}$ RECs.

The various transcriptome comparisons described above reflect Norrin/Fz4/Lrp signaling in different contexts: the yolk sac contains actively proliferating and differentiating embryonic vasculature; the WT or mutant adult retinal vasculature is enriched in or depleted of capillaries, respectively; and REC culture experiments reveal responses ex vivo. It is noteworthy that the two transcripts with abundance changes that correlate most consistently ($P<0.01$) with increased Fz4/Lrp signaling code for SparcL1/Hevin/SC1/MAST9, an ECM-associated protein implicated in vascular remodeling (Girard and Springer, 1996; Barker et al., 2005), and Sox17 (Figure 7D).

Sox17 mediates Norrin/Fz4/Lrp-dependent production of capillary-like structures

Our observation that the abundance of *Sox17* transcripts is increased by Norrin/Fz/Lrp signaling in a variety of contexts (Figure 7A–C) led us to ask whether production of Sox17 alone might rescue the defect exhibited by *Fz4*$^{-/-}$ RECs in Matrigel. To this end, multiple stable cell lines were generated by infecting *Fz4*$^{-/-}$ REC lines with a lentivirus vector expressing Sox17. RNA blotting showed that *Sox17* transcripts are readily detectable in WT RECs, undetectable in parental *Fz4*$^{-/-}$ RECs, and present at roughly WT levels in the lentivirus-Sox17-transduced derivatives of *Fz4*$^{-/-}$ RECs (Figure 7E). Matrigel assays with 11 cloned Sox17-transduced lines and pools of Sox17-transduced cells derived from three *Fz4*$^{-/-}$ REC

lines revealed, in every case, a restoration of WT levels of capillary-like structures (Figure 7F). Thus, Sox17 appears to be a principal mediator of the angiogenic program controlled by Norrin/Fz4/Lrp signaling.

DISCUSSION

The results described here establish Norrin/Fz4/Lrp signaling as a central regulator of REC development, and they indicate that the hypovascularization responsible for Norrie disease, FEVR, and osteoporosis-pseudoglioma syndrome arises from the impairment of a specific transcriptional program. They also suggest that Fz4/Lrp signaling could play a role in vascular growth, remodeling, and maintenance in a variety of normal and pathologic contexts beyond the retina.

The relationship between retinal and hyaloid vasculatures

Our data distinguish between several competing hypotheses regarding the origins of retinal hypovascularization in $Fz4^{-/-}$, $Lrp5^{-/-}$, and Ndp^{-} mice (Kato et al., 2002; Ohlmann et al., 2004). In particular, the highly localized defects in vascular structure in mosaic $Fz4^{CKOAP/-}$*;Tie2-Cre* retinas and the failure of $Fz4^{-/-}$ RECs to form capillary-like structures in vitro are inconsistent with the hypothesis that retinal hypovascularization in $Fz4^{-/-}$, $Lrp5^{-/-}$, and Ndp^{-} mice is secondary to inappropriate expansion and preservation of the hyaloid vasculature (a transient vascular structure within the vitreous cavity), which then increases retinal oxygenation and suppresses retinal vascularization. Instead, our data favor the opposite causal sequence: that the primary defect in $Fz4^{-/-}$, $Lrp5^{-/-}$, and Ndp^{-} mice is retinal hypovascularization, and the expansion and delayed regression of the hyaloid vasculature is a secondary consequence of retinal hypoxia. Our data also rule out models positing that the primary defect in Norrin/Fz4/Lrp signaling arises in RGCs, astrocytes, or other cells that guide vascular growth.

Control of vascular gene regulation and development by Norrin/Fz4/Lrp signaling

The present study presents a genome-wide analysis of transcripts in the retinal vasculature, and it reveals several hundred transcripts with substantial changes in response to Norrin/Fz4 signaling, including *Sox17* transcripts. In mice, Sox17 and Sox18 act in a partially redundant manner to promote angiogenesis (Matsui et al., 2006; Sakamoto et al., 2007), and Wnt/beta-catenin signaling in differentiating ES cells leads to induction of Sox17 transcripts in developing endoderm and cardiac mesoderm (Liu et al., 2007). The demonstration that Sox17 rescues the Matrigel phenotype of $Fz4^{-/-}$ RECs implies that Fz4/Lrp signaling in ECs activates a Sox17-dependent program that produces exploratory, migratory, and adhesive behaviors.

Using the Ndp^{AP} mouse we have demonstrated that *Ndp* is expressed principally in Muller glia. However, the ability of a Norrin transgene with lens-specific expression to rescue the Ndp^{-} retinal vascular phenotype argues that a precisely localized source is not essential for Norrin action (Ohlmann et al., 2005). Thus, Norrin/Fz4/Lrp signaling likely affects EC behavior at the level of cell competence rather than by acting directly as a chemo-attractant.

Minimal overlap of retinal vascular territories

The preservation of photoreceptor light responses and the loss of signal transmission in the inner retina in Ndp^{-} retinas (Luhmann et al., 2005b) and in $Fz4^{-/-}$ and $Fz4^{CKOAP/-}$*;Tie2-Cre* retinas (this work) supports the existence of a sharp boundary between the territories served by the choroidal and retinal vasculatures, which supply the photoreceptors and the inner retina, respectively (Alm, 1992). Similarly, the normal functioning of intrinsically photosensitive RGCs in $Fz4^{-/-}$ and $Fz4^{CKOAP/-}$*;Tie2-Cre* mice indicates a sharp boundary between the territories supplied by blood vessels at the vitreal face of the retina (RGC layer) and by

intraretinal capillaries (inner nuclear layer). In *Fz4*$^{-/-}$ retinas, defective signal transmission appears to arise from a partially reversible hypoxia, acidosis, or related metabolic derangement, rather than from irreversible damage. This finding implies that some neurons may be able to survive extended periods of hypo-perfusion, and that functional losses in some CNS vascular diseases, even over an extended time period, could be partially reversible.

Implications of Norrin/Fz4/Lrp signaling for retinal vascular diseases

It is intriguing to consider the possibility that Norrin/Fz4/Lrp signaling might be relevant to retinal vascular diseases such as diabetic retinopathy or retinopathy of prematurity. The continued expression of *Norrin*, *Fz4*, and *Lrp5* in the mature retina and the identification of *NDP* mutations in a few individuals with retinopathy of prematurity (Shastry et al., 1997) suggest that there may be a role for Norrin/Fz4/Lrp signaling in pathologic retinal vascular remodeling. Finally, the observations that some humans with *NDP* mutations exhibit peripheral venous insufficiency (Rehm et al., 1997; Michaelides et al., 2004), that *Fz4* is expressed throughout the vasculature and is required for vascular integrity in the cerebellum (this study), that Fz4 and Norrin are required to maintain the capillaries of the stria vascularis (Rehm et al., 2002; Xu et al., 2004), and that Fz4 and Norrin are required for female fertility (Hsieh et al., 2005; Luhmann et al., 2005a), together suggest a wider role for this signaling system in vascular biology and disease.

EXPERIMENTAL PROCEDURES

Gene Targeting

The *Fz4*^{CKOAP}, *Z/Norrin*, *Ndp*$^{-}$, and *Ndp*^{AP} alleles were created by standard gene targeting methods.

Micro-array hybridization

RNA samples were labeled with either the GeneChip© Expression 3′ Amplification One Cycle Target Labeling Kit (P/N 900493; for 1–5ug RNA samples), or the Ovation RNA amplification System V2 (P/N 3100; for ~0.1 ug RNA samples) and FL-Ovation cDNA Biotin Module V2 (P/N 4200) kits (Nugen). The labeled probes were hybridized to Affymetrix mouse 430 2.0 chips, and micro-array data were analyzed with Spotfire software.

Vascular cell purification and REC culture

Immuno-purification and cell culture was performed as described in Su et al. (2003).

Scratch wound and Matrigel assays

Scratch wounds were made by drawing a 1 ml pipette tip across the surface of a confluent REC monolayer. Matrigel assays were performed in DMEM with 1% FBS for 6–8 hours at 37°C. For mixed cultures, RECs were first incubated with 0.3% DiI or DiO.

Optokinetic reflex (OKR) and pupillary light responses

OKR measurements were performed as described in Cahill and Nathans (2008). To measure pupil responses, the chamber was maintained in complete darkness for 30 seconds, followed by 30 seconds of constant bright light (400 lux).

Multi-electrode array (MEA) recordings

The MEA hardware and MCRack software (Multi Channel Systems, Reutlingen, Germany; distributed by ALA Scientific) and recording protocols are similar to those described by Meister et al. (1994). Voltages were recorded from the 60 electrodes at 25,000 Hz and analyzed

using MATLAB with routines based on the FIND 1.0 Toolbox [University of Freiburg (http://find.bccn.uni-freiburg.de/)]. Spikes were sorted by morphology using the K-means algorithm with 1, 2, 3, or 4 clusters, and for each K-means cluster at each electrode the peri-stimulus histograms for the 25 stimulus locations was calculated. Division into ON, OFF, and ON-OFF response classes was determined by calculating an ON vs. OFF index based on the spike frequencies in the light and dark portions of the stimulus train [(spike frequency in light – spike frequency in darkness)/(spike frequency in light + spike frequency in darkness)]. The range of this index is −1 (exclusively OFF) to +1 (exclusively ON), and cells were categorized as ON, ON-OFF, or OFF if their index values were >0.3, between −0.3 and +0.3, or <−0.3, respectively.

Supplementary Material

Refer to Web version on PubMed Central for supplementary material.

Acknowledgments

The authors thank Elke Stein, Shin Kang, and Dwight Bergles for helpful discussions; Chip Hawkins and the JHMI transgenic core for blastocyst injection; Lawrence Chan, Milan Jamrich, Eric Swindell, Ralf Adams, and Masashi Yanagisawa for mouse lines; Se-Jin Lee for the mouse ES cell genomic library; Huimin Yu for the Norrin-expressing 293 cell line; Corrinne Lobe for the *Z/AP* plasmid; William Guggino for the use of his fluorescent microscope; Hongjun Song for advice on producing the lentivirus; Linda Orzolek, Ira Maine, Haiping Hao and Connie Talbot for micro-array support; Yifeng Zhang and Markus Meister for advice on micro-electrode array recording; and David Ginty, Stewart Hendry, Se-Jin Lee, Amir Rattner, and Randy Reed for helpful comments on the manuscript. Supported by the National Eye Institute and the Howard Hughes Medical Institute.

References

Adams RH, Alitalo K. Molecular regulation of angiogenesis and lymphangiogenesis. Nat Rev Mol Cell Biol 2007;8:464–478. [PubMed: 17522591]

Ai M, Heeger S, Bartels CF, Schelling DK. Osteoporosis-Pseudoglioma Collaborative Group. Clinical and molecular findings in osteoporosis-pseudoglioma syndrome. Am J Hum Genet 2005;77:741–53. [PubMed: 16252235]

Alm, A. Ocular circulation. In: Hart, WM., editor. Adler's Physiology of the Eye. Vol. 9. Saint Louis: Mosby; 1992. p. 198-227.

Armulik A, Abramsson A, Betsholtz C. Endothelial/pericyte interactions. Circ Res 2005;97:512–523. [PubMed: 16166562]

Barker TH, Framson P, Puolakkainen PA, Reed M, Funk SE, Sage EH. Matricellular homologs in the foreign body response: hevin suppresses inflammation, but hevin and SPARC together diminish angiogenesis. Am J Pathol 2005;166:923–33. [PubMed: 15743803]

Berger, W.; Ropers, HH. Norrie Disease. In: Scriver, CR.; Beaudet, AL.; Sly, WS.; Valle, D., editors. Metabolic and Molecular Bases of Inherited Disease. Vol. 8. New York: McGraw Hill; 2001. p. 5977-5985.

Cahill H, Nathans J. The optokinetic reflex as a tool for quantitative analysis of nervous system function in mice: application to genetic and drug-induced variation. PLoS One 2008;3:e2055. [PubMed: 18446207]

Daneman R, Agalliu D, Zhou L, Kuhnert F, Kuo CJ, Barres BA. Wnt/beta-catenin signaling is required for CNS, but not non-CNS, angiogenesis. Proc Natl Acad Sci USA 2009;106:641–6. [PubMed: 19129494]

Foo SS, Turner CJ, Adams S, Compagni A, Aubyn D, Kogata N, Lindblom P, Shani M, Zicha D, Adams RH. Ephrin-B2 controls cell motility and adhesion during blood-vessel-wall assembly. Cell 2006;124:161–173. [PubMed: 16413489]

Gariano RF, Gardner TW. Retinal angiogenesis in development and disease. Nature 2005;438:960–966. [PubMed: 16355161]

Girard JP, Springer TA. Modulation of endothelial cell adhesion by hevin, an acidic protein associated with high endothelial venules. J Biol Chem 1996;271:4511–4517. [PubMed: 8626806]

Hattar S, Lucas RJ, Mrosovsky N, Thompson S, Douglas RH, Hankins MW, Lem J, Biel M, Hofmann F, Foster RG, Yau KW. Melanopsin and rod-cone photoreceptive systems account for all major accessory visual functions in mice. Nature 2003;424:76–81. [PubMed: 12808468]

Hayashi S, Lewis P, Pevny L, McMahon AP. Efficient gene modulation in mouse epiblast using a Sox2Cre transgenic mouse strain. Gene Exp Patterns 2002;2:93–97.

Hsieh M, Boerboom D, Shimada M, Lo Y, Parlow AF, Luhmann UF, Berger W, Richards JS. Mice null for Frizzled4 (Fzd4−/−). are infertile and exhibit impaired corpora lutea formation and function. Biol Reprod 2005;73:1135–1146. [PubMed: 16093361]

Iwakabe H, Katsuura G, Ishibashi C, Nakanishi S. Impairment of pupillary responses and optokinetic nystagmus in the mGluR6-deficient mouse. Neuropharmacology 1997;36:135–143. [PubMed: 9144650]

Jat PS, Noble MD, Ataliotis P, Tanaka Y, Yannoutsos N, Larsen L, Kioussis D. Direct derivation of conditionally immortal cell lines from an H-2Kb-tsA58 transgenic mouse. Proc Natl Acad Sci USA 1991;88:5096–5100. [PubMed: 1711218]

Jiao X, Ventruto V, Trese MT, Shastry BS, Hejtmancik JF. Autosomal recessive familial exudative vitreoretinopathy is associated with mutations in LRP5. Am J Hum Genet 2004;75:878–884. [PubMed: 15346351]

Kato M, Patel MS, Levasseur R, Lobov I, Chang BH, Glass DA 2nd, Hartmann C, Li L, Hwang TH, Brayton CF, Lang RA, Karsenty G, Chan L. Cbfa1-independent decrease in osteoblast proliferation, osteopenia, and persistent embryonic eye vascularization in mice deficient in Lrp5, a Wnt coreceptor. J Cell Biol 2002;157:303–314. [PubMed: 11956231]

Kisanuki YY, Hammer RE, Miyazaki J, Williams SC, Richardson JA, Yanagisawa M. Tie2-Cre transgenic mice: a new model for endothelial cell-lineage analysis in vivo. Dev Biol 2001;230:230–242. [PubMed: 11161575]

Kondo H, Qin M, Tahira T, Uchio E, Hayashi K. Severe form of familial exudative vitreoretinopathy caused by homozygous R417Q mutation in frizzled-4 gene. Ophthalmic Genet 2007;28:220–223. [PubMed: 18161623]

Liu Y, Asakura M, Inoue H, Nakamura T, Sano M, Niu Z, Chen M, Schwartz RJ, Schneider MD. Sox17 is essential for the specification of cardiac mesoderm in embryonic stem cells. Proc Natl Acad Sci USA 2007;104:3859–3864. [PubMed: 17360443]

Lobe CG, Koop KE, Kreppner W, Lomeli H, Gertsenstein M, Nagy A. Z/AP, a double reporter for cre-mediated recombination. Dev Biol 1999;208:281–292. [PubMed: 10191045]

Luhmann UF, Meunier D, Shi W, Lüttges A, Pfarrer C, Fundele R, Berger W. Fetal loss in homozygous mutant Norrie disease mice: a new role of Norrin in reproduction. Genesis 2005a;42:253–262. [PubMed: 16035034]

Luhmann UF, Lin J, Acar N, Lammel S, Feil S, Grimm C, Seeliger MW, Hammes HP, Berger W. Role of the Norrie disease pseudoglioma gene in sprouting angiogenesis during development of the retinal vasculature. Invest Ophthalmol Vis Sci 2005b;46:3372–3382. [PubMed: 16123442]

Luhmann UF, Neidhardt J, Kloeckener-Gruissem B, Schäfer NF, Glaus E, Feil S, Berger W. Vascular changes in the cerebellum of Norrin/Ndph knockout mice correlate with high expression of Norrin and Frizzled-4. Eur J Neurosci 2008;27:2619–2628. [PubMed: 18547247]

Matsui T, Kanai-Azuma M, Hara K, Matoba S, Hiramatsu R, Kawakami H, Kurohmaru M, Koopman P, Kanai Y. Redundant roles of Sox17 and Sox18 in postnatal angiogenesis in mice. J Cell Sci 2006;119:3513–3526. [PubMed: 16895970]

McCall MA, Gregg RG. Comparisons of structural and functional abnormalities in mouse b-wave mutants. J Physiol 2008;586:4385–4392. [PubMed: 18653656]

Meister M, Pine J, Baylor DA. Multi-neuronal signals from the retina: acquisition and analysis. J Neurosci Methods 1994;51:95–106. [PubMed: 8189755]

Michaelides M, Luthert PJ, Moore AT, Cooling R, Firth H. Norrie disease and peripheral venous insufficiency. Br J Ophthalmol 2004;88:1475. [PubMed: 15489496]

Ohlmann AV, Adamek E, Ohlmann A, Lütjen-Drecoll E. Norrie gene product is necessary for regression of hyaloid vessels. Invest Ophthalmol Vis Sci 2004;45:2384–2390. [PubMed: 15223821]

Ohlmann A, Scholz M, Goldwich A, Chauhan BK, Hudl K, Ohlmann AV, Zrenner E, Berger W, Cvekl A, Seeliger MW, Tamm ER. Ectopic norrin induces growth of ocular capillaries and restores normal retinal angiogenesis in Norrie disease mutant mice. J Neurosci 2005;25:1701–1710. [PubMed: 15716406]

Pendeville H, Winandy M, Manfroid I, Nivelles O, Motte P, Pasque V, Peers B, Struman I, Martial JA, Voz ML. Zebrafish Sox7 and Sox18 function together to control arterial-venous identity. Dev Biol 2008;317:405–416. [PubMed: 18377889]

Qin M, Hayashi H, Oshima K, Tahira T, Hayashi K, Kondo H. Complexity of the genotype-phenotype correlation in familial exudative vitreoretinopathy with mutations in the LRP5 and/or FZD4 genes. Hum Mutat 2005;26:104–112. [PubMed: 15981244]

Rehm HL, Gutierrez-Espeleta GA, Garcia R, Jimenez G, Khetarpal U, Priest JM, Sims KB, Keats BJ, Morton CC. Norrie disease gene mutation in a large Costa Rican kindred with a novel phenotype including venous insufficiency. Hum Mutation 1997;9:402–408.

Rehm HL, Zhang DS, Brown MC, Burgess B, Halpin C, Berger W, Morton CC, Corey DP, Chen ZY. Vascular defects and sensorineural deafness in a mouse model of Norrie disease. J Neurosci 2002;22:4286–4292. [PubMed: 12040033]

Richter M, Gottanka J, May CA, Welge-Lüssen U, Berger W, Lütjen-Drecoll E. Retinal vasculature changes in Norrie disease mice. Invest Ophthalmol Vis Sci 1998;39:2450–2457. [PubMed: 9804153]

Robitaille J, MacDonald ML, Kaykas A, Sheldahl LC, Zeisler J, Dube MP, Zhang LH, Singaraja RR, Guernsey DL, Zheng B, Siebert LF, Hoskin-Mott A, Trese MT, Pimstone SN, Shastry BS, Moon RT, Hayden MR, Goldberg YP, Samuels ME. Mutant frizzled-4 disrupts retinal angiogenesis in familial exudative vitreoretinopathy. Nat Genet 2002;32:326–330. [PubMed: 12172548]

Sakamoto Y, Hara K, Kanai-Azuma M, Matsui T, Miura Y, Tsunekawa N, Kurohmaru M, Saijoh Y, Koopman P, Kanai Y. Redundant roles of Sox17 and Sox18 in early cardiovascular development of mouse embryos. Biochem Biophys Res Commun 2007;360:539–544. [PubMed: 17610846]

Schlaeger TM, Qin Y, Fujiwara Y, Magram J, Sato TN. Vascular endothelial cell lineage-specific promoter in transgenic mice. Development 1995;121:1089–1098. [PubMed: 7743922]

Shastry BS, Pendergast SD, Hartzer MK, Liu X, Trese MT. Identification of missense mutations in the Norrie disease gene associated with advanced retinopathy of prematurity. Arch Ophthalmol 1997;115:651–655. [PubMed: 9152134]

Smallwood PM, Williams J, Xu Q, Leahy DJ, Nathans J. Mutational analysis of Norrin-Frizzled4 recognition. J Biol Chem 2007;282:4057–4068. [PubMed: 17158104]

Stenman JM, Rajagopal J, Carroll TJ, Ishibashi M, McMahon J, McMahon AP. Canonical Wnt signaling regulates organ-specific assembly and differentiation of CNS vasculature. Science 2008;322:1247–1250. [PubMed: 19023080]

Su X, Sorenson CM, Sheibani N. Isolation and characterization of murine retinal endothelial cells. Mol Vision 2003;9:171–178.

Swindell EC, Bailey TJ, Loosli F, Liu C, Amaya-Manzanares F, Mahon KA, Wittbrodt J, Jamrich M. Rx-Cre, a tool for inactivation of gene expression in the developing retina. Genesis 2006;44:361–363. [PubMed: 16850473]

Toomes C, Bottomley HM, Jackson RM, Towns KV, Scott S, Mackey DA, Craig JE, Jiang L, Yang Z, Trembath R, Woodruff G, Gregory-Evans CY, Gregory-Evans K, Parker MJ, Black GC, Downey LM, Zhang K, Inglehearn CF. Mutations in LRP5 or FZD4 underlie the common familial exudative vitreoretinopathy locus on chromosome 11q. Am J Hum Genet 2004;74:721–730. [PubMed: 15024691]

Wang Y, Huso D, Cahill H, Ryugo D, Nathans J. Progressive cerebellar, auditory, and esophageal dysfunction caused by targeted disruption of the frizzled-4 gene. J Neurosci 2001;21:4761–4771. [PubMed: 11425903]

Xia CH, Liu H, Cheung D, Wang M, Cheng C, Du X, Chang B, Beutler B, Gong X. A model for familial exudative vitreoretinopathy caused by LPR5 mutations. Hum Mol Genet 2008;17:1605–1612. [PubMed: 18263894]

Xu Q, Wang Y, Dabdoub A, Smallwood PM, Williams J, Woods C, Kelley MW, Jiang L, Tasman W, Zhang K, Nathans J. Vascular development in the retina and inner ear: control by Norrin and Frizzled-4, a high-affinity ligand-receptor pair. Cell 2004;116:883–895. [PubMed: 15035989]

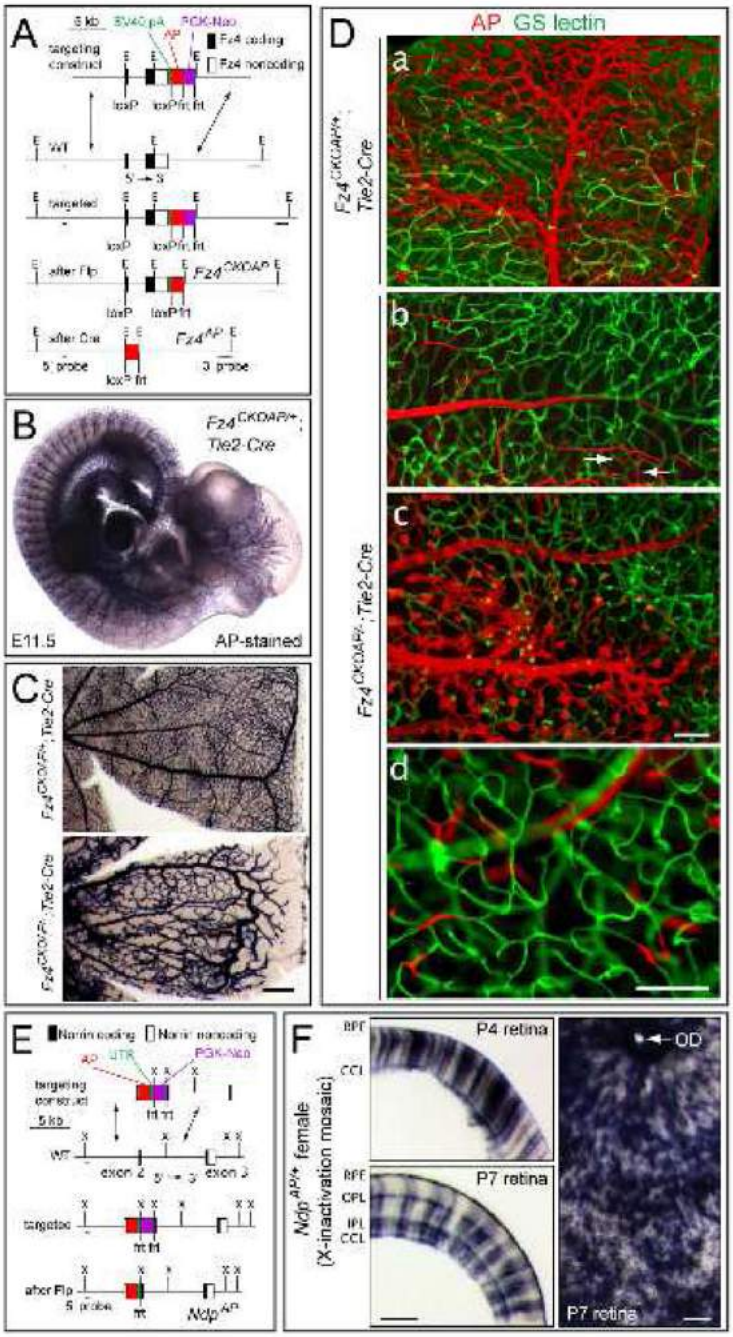

Figure 1.

Expression of *Fz4* in ECs and *Ndp* in Muller glia: absence of *Fz4* signaling in ECs leads to severe defects in retinal vascular development.

(A) Structure of the $Fz4^{CKOAP}$ allele. *LoxP* sites were placed in the 5′ UTR and 3′ of the 3′ UTR. Cre-mediated recombination deletes *Fz4* coding sequences and activates AP. E, *Eco*R I.

(B) *Fz4* is expressed in ECs as determined by AP histochemistry of a $Fz4^{CKOAP/+}$;*Tie2-Cre* E11.5 embryo.

(C) AP histochemistry of adult retinas. $Fz4^{AP/+}$ ECs produce a WT vasculature, and $Fz4^{AP/-}$ ECs produce a vascular phenotype identical to that of $Fz4^{-/-}$ mice. Scale bar, 200 um.

(D) Mosaic analysis of *Fz4*$^{CKOAP/+}$*;Tie2-Cre* and *Fz4*$^{CKOAP/-}$;*Tie2-Cre* retinas with incomplete Cre-mediated recombination. a, *Fz4*$^{AP/+}$ ECs populate large vessels and capillaries. b–d, vessels are populated by *Fz4*$^{AP/-}$ ECs only if they reside on the vitreal surface (b and c); intraretinal growth of *Fz4*$^{AP/-}$ ECs typically ends in a compact ball of cells (c), with some *Fz4*$^{AP/-}$ ECs incorporated into the adjacent WT capillary network (white arrows in b). d, rare *Tie2-Cre*-mediated recombination events generate isolated *Fz4*$^{AP/-}$ ECs within mature intra-retinal capillaries. Scale bar, 100 um.

(E) Structure of the *Ndp*^{AP} allele. UTR, rabbit beta-globin 3′ UTR; X, *Xba* I.

(F) AP-stained retinas from *Ndp*$^{AP/+}$ female mice. 40 um cross-sections at P4 and P7 (left) and a flat mount at P7 (right). AP+ Muller glia span the full thickness of the retina. The brown dots in the flat mount are adherent RPE cells. Scale bars, 100 um. RPE, retinal pigment epithelium; OPL, outer plexiform layer; IPL, inner plexiform layer, GCL, ganglion cell layer; OD, optic disc.

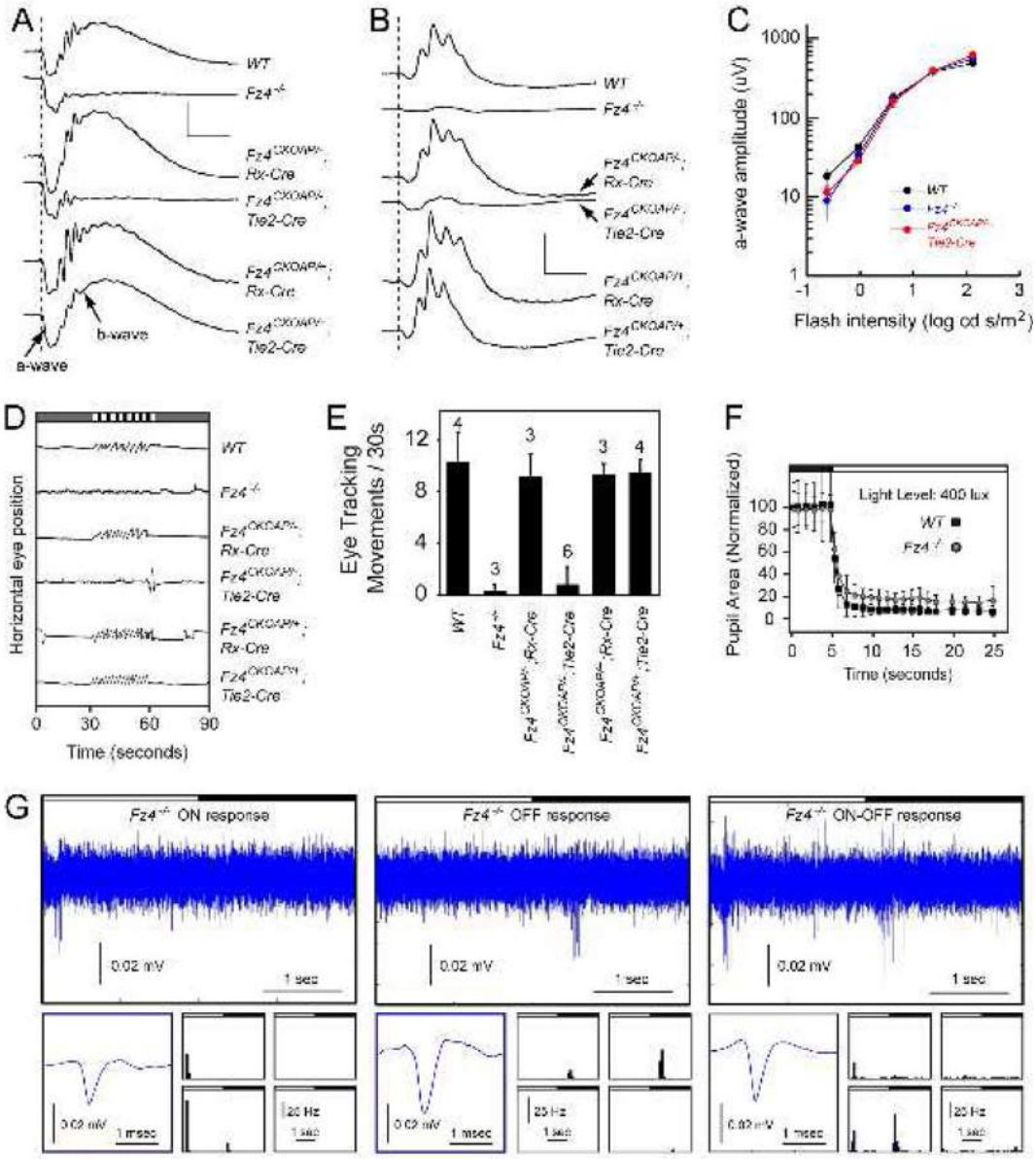

Figure 2.

Deficits in visual function associated with retinal vascular insufficiency

(A) Rod ERG responses to a strobe flash (dashed line) presented in darkness. Scale bars, 500 **u**V and 50 ms.

(B) Cone ERG responses to a strobe flash (dashed line) superimposed upon a steady rod-desensitizing adapting field. Scale bars, 200 **u**V and 50 ms.

(C) Amplitude of the dark-adapted a-wave measured 8 ms after the flash, as a function of stimulus intensity. There is no statistically significant difference between control a-waves (averages of *Fz4*$^{+/+}$, Fz4$^{+/-}$, Fz4$^{CKOAP/+}$;Rx-Cre, and Fz4$^{CKOAP/+}$;Tie2-Cre) and Fz4$^{-/-}$ and Fz4$^{CKOAP/-}$*;Tie2-Cre* a-waves. The number of mice tested were: *Fz4*$^{+/+}$ (2), *Fz4*$^{+/-}$ (4), Fz4$^{CKOAP/+}$;Rx-Cre (6), Fz4$^{CKOAP/+}$;Tie2-Cre mice (5), Fz4$^{-/-}$ (7), Fz4$^{CKOAP/-}$;Rx-Cre (6), and Fz4$^{CKOAP/-}$;Tie2-Cre (6). Bars, SD.

(D) The OKR to horizontally rotating vertical stripes (striped bar at top) is lost in *Fz4*$^{-/-}$ and *Fz4*$^{CKOAP/-}$*;Tie2-Cre* mice.

(E) Quantification of the OKR. The number of mice tested is indicated. Among six *Fz4*$^{CKOAP/-}$*;Tie2-Cre* tested, one showed a weak OKR and was subsequently found to exhibit incomplete Cre-mediated recombination in the retinal vasculature; the remaining five mice showed no OKR. Bars, SD.

(F) *Fz4*$^{-/-}$ and WT littermates show nearly normal pupil constriction following the onset of a 400 lux stimulus (open bar at top). For each genotype, four mice were tested six times and the 24 responses averaged. Bars, SD.

(G) Extracellular multi-electrode array recordings of light responses from ganglion cell layer neurons from two month old *Fz4*$^{-/-}$ retinas. Upper panels, individual ON, OFF, and ON-OFF cell responses to two seconds of light followed by two seconds of darkness (black and white bars). Shown for each cell is the averaged spike waveform obtained from ten repetitions of the alternating light/dark stimulus (lower left panels) and a peri-stimulus histogram showing the frequency (Hz) and timing of spikes in response to ten repetitions of the stimulus at each of four stimulus locations comprising a 2×2 subset of the 5×5 stimulus array (lower panels; 100 msec bins).

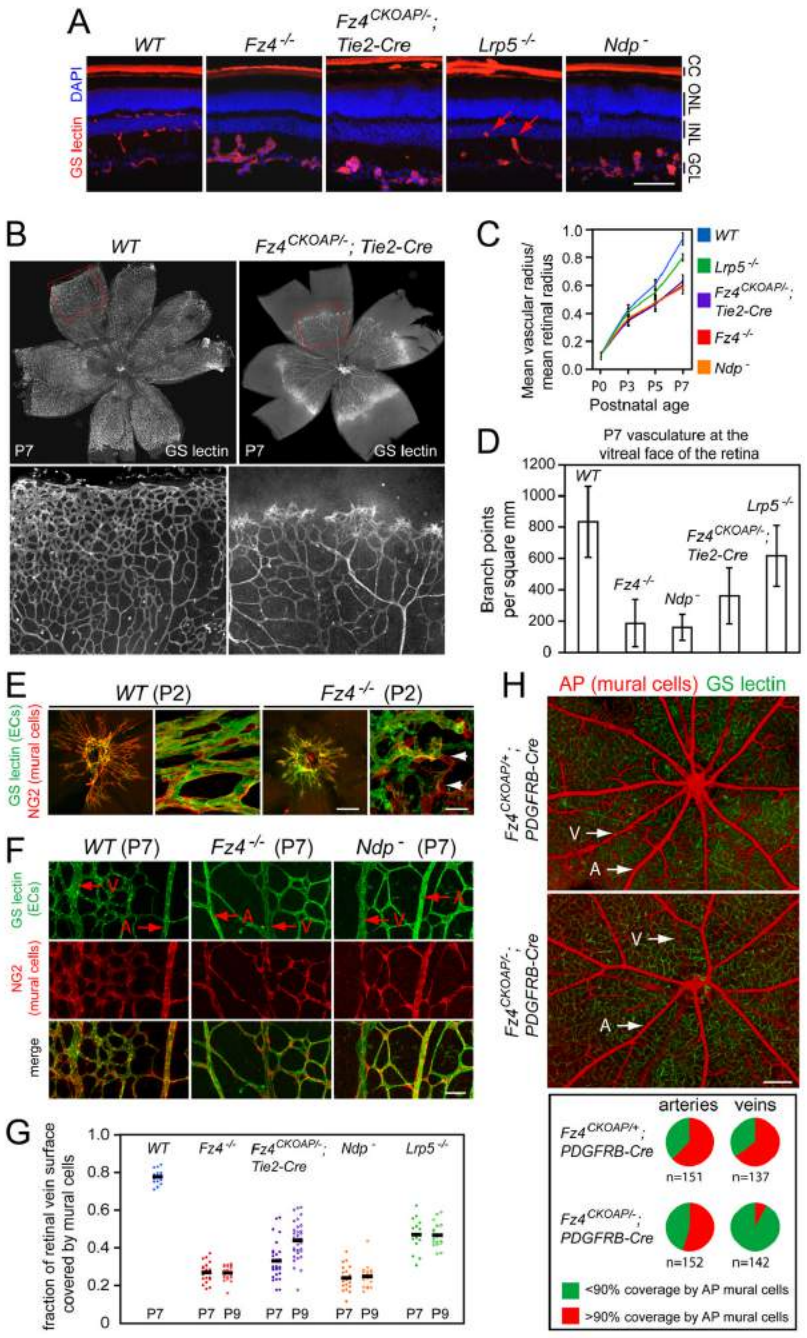

Figure 3.

Fz4 signaling is required for retinal vascular growth and for normal EC-MC interactions.

(A) WT adult retina show the normal two tiers of capillaries. *Fz4*$^{-/-}$, *Fz4*$^{CKOAP/-}$*;Tie2-Cre*, and *Ndp*$^{-}$ retinas fail to develop intraretinal capillaries; *Lrp5*$^{-/-}$ retinas show partial development of the inner tier (red arrows). CC, choriocapillaris; ONL, outer nuclear layer; INL, inner nuclear layer; GCL, ganglion cell layer. Scale bar, 100 um.

(B) Delayed EC migration and impoverished vascular network formation in *Fz4*$^{CKOAP/-}$*;Tie2-Cre* retinas at P7. Regions boxed in red are shown at higher magnification; the vessels reside on the vitreal surface. Scale bar, 20 um.

(C) Quantification of EC spreading from the optic disc. *Fz4*$^{-/-}$, *Fz4*$^{CKOAP/-}$*;Tie2-Cre*, and *Ndp*$^{-}$ retinas are equivalently defective; *Lrp5*$^{-/-}$ retinas show a milder defect. For each genotype, 6–10 retinas were analyzed per time point. Bars, SEM.
(D) Quantification of vascular density at the vitreal surface. *Lrp5*$^{-/-}$retinas show a mild defect, *Fz4*$^{CKOAP/-}$*;Tie2-Cre* retinas show an intermediate defect, and *Fz4*$^{-/-}$ and *Ndp*$^{-}$ retinas show equivalently severe defects. Bars, SEM.
(E) P2 retina flat mounts show that MC coverage of ECs in *Fz4*$^{-/-}$ retinas is aberrant from the earliest stages of vascular development (white arrows, detached MCs). a,c, images centered at the optic disc; scale bar, 200 um. b,d, scale bar 20 um.
(F) P7 retina flat mounts show decreased MC coverage of capillaries and veins (V), with minimal affect on arteries (A), in *Fz4*$^{-/-}$ and *Ndp*$^{-}$ retinas. Scale bar, 50 um.
(G) Quantification of the surface area of the principal retinal veins covered by MCs. Mutant retinas were examined at P7 and P9 because vascular migration is delayed ~2 days (Figure 3B and C). Each data point represents a different vein. Black bars, averages. P7 vs. P9 *Fz4*$^{CKOAP/-}$*;Tie2-Cre* ($p<0.0001$, student t-test); P9 *Fz4*$^{CKOAP/-}$*;Tie2-Cre* vs. *Fz4*$^{-/-}$ or *Norrin*$^{-}$ ($p<0.0001$, ANOVA). Each mutant at either P7 or P9 vs. WT at P7 ($p<0.0001$, student t-test).
(H) *Fz4*$^{AP/+}$ and *Fz4*$^{AP/-}$ MCs visualized at P30 in the *Fz4*$^{CKOAP/+}$*;PDGFRB-Cre* retina (upper panel) and *Fz4*$^{CKOAP/-}$*;PDGFRB-Cre* retina (lower panel), respectively. GS-lectin staining shows normal capillary architecture in both retinas. Recombination is more efficient in MCs on large vessels compared to capillaries. Pie charts show MC coverage at P30, with the number of scored veins and arteries indicated. The artery coverage difference is not statistically significant ($P=0.162$); for the vein coverage, $P=10^{-25}$ (Fisher's exact test). Scale bar, 200 um.

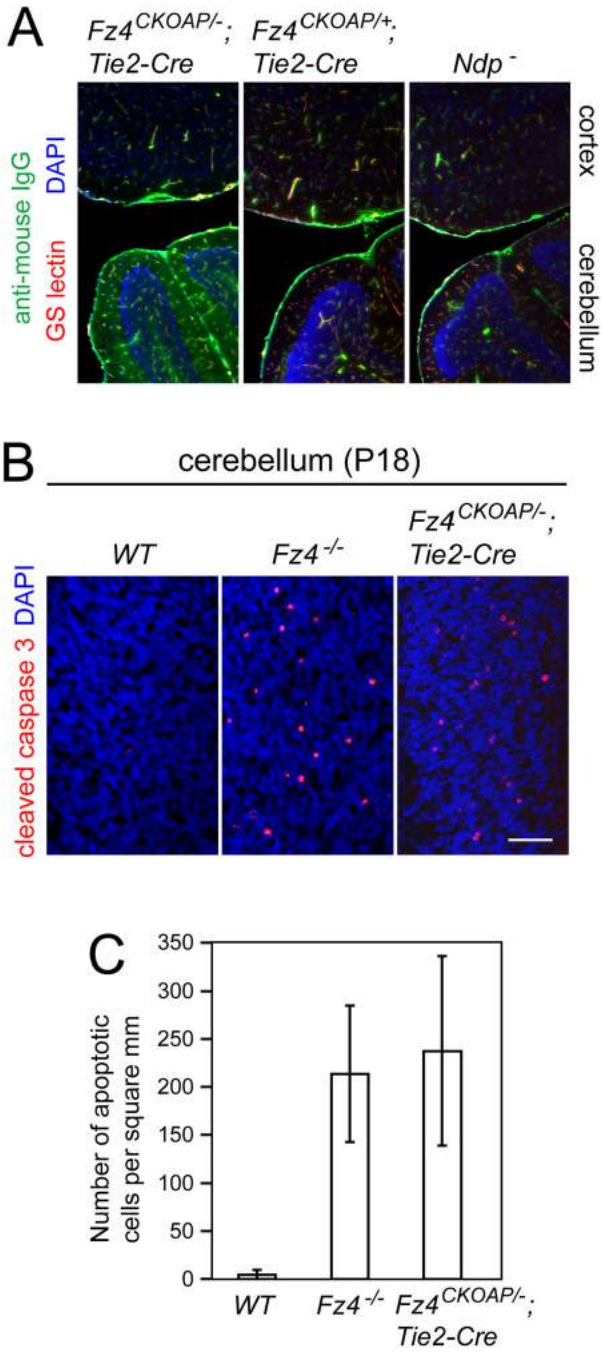

Figure 4.

Vascular basis of cerebellar degeneration in *Fz4*$^{-/-}$ mice.

(A) Loss of vascular integrity occurs in the *Fz4*$^{CKOAP/-}$;*Tie2-Cre* cerebellum but not cerebral cortex as determined by staining for IgG in freshly frozen tissue. Scale bar, 300 um.

(B,C) Large numbers of apoptotic granule cells in the P18 cerebellum are observed with deletion of *Fz4* in ECs. P<10^{-6} for *Fz4*$^{CKOAP/-}$;*Tie2-Cre* vs. WT and for *Fz4*$^{-/-}$ vs. WT (student t-test). Scale bar in B, 50 um. Bars, SEM.

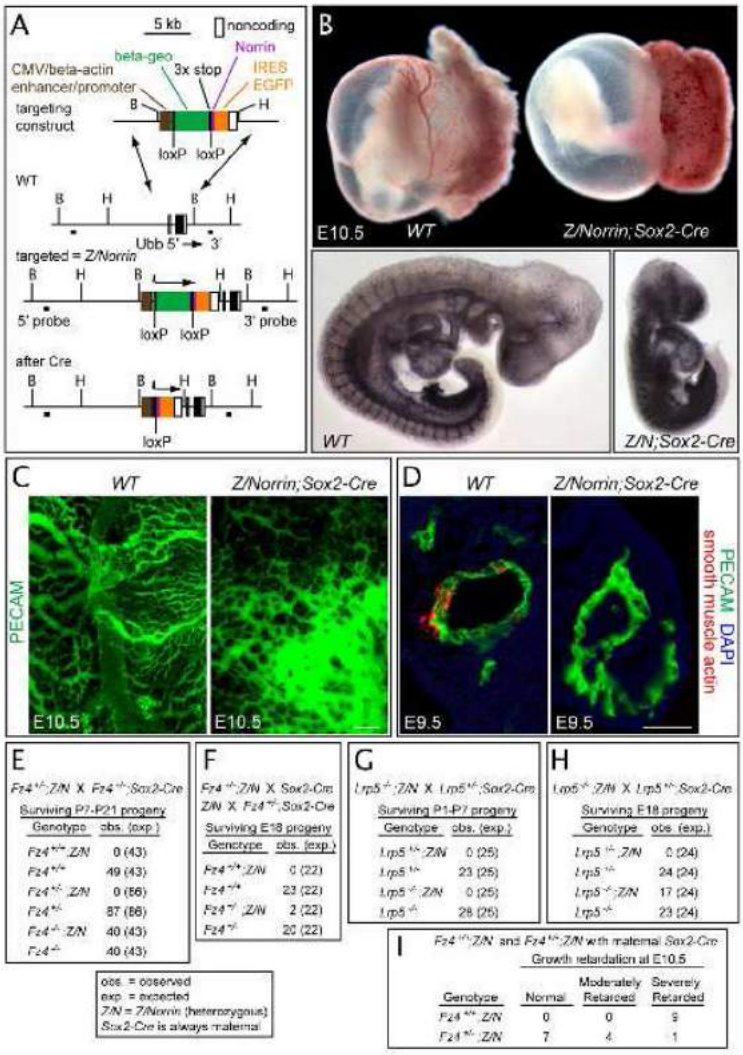

Figure 5.

Ubiquitous production of Norrin during embryogenesis leads to vascular disorganization

(A) Targeted insertion of a Cre-activated Norrin expression cassette upstream of the *Ubb* gene. Cre-mediated recombination eliminates a *loxP*-flanked *beta-geo* and three transcription termination sites, permitting transcription of *Norrin-IRES-EGFP*.

(B) Upper panel, *Z/Norrin;Sox2-Cre* embryos have a severe defect in yolk sac vascular development and retarded embryonic growth at E10.5. Lower panels, anti-PECAM immunostaining at E10.5 shows generalized vascular disorganization in a *Z/Norrin;Sox2-Cre* embryo (right).

(C) Flat-mounted E10.5 yolk sacs show an orderly hierarchy of vessel sizes in WT (left), and undeveloped and disorganized vasculature in a *Z/Norrin;Sox2-Cre* yolk sac (right). Scale bar, 200 um.

(D) Dorsal aorta at E9.5. vSMCs are absent in the *Z/Norrin;Sox2-Cre* aorta. Scale bar, 50 um.

(E–I) Lethality caused by ubiquitous Norrin production is suppressed in a $Fz4^{-/-}$ background (E), and partially suppressed in $Fz4^{+/-}$ and $Lrp5^{-/-}$backgrounds (F–I).

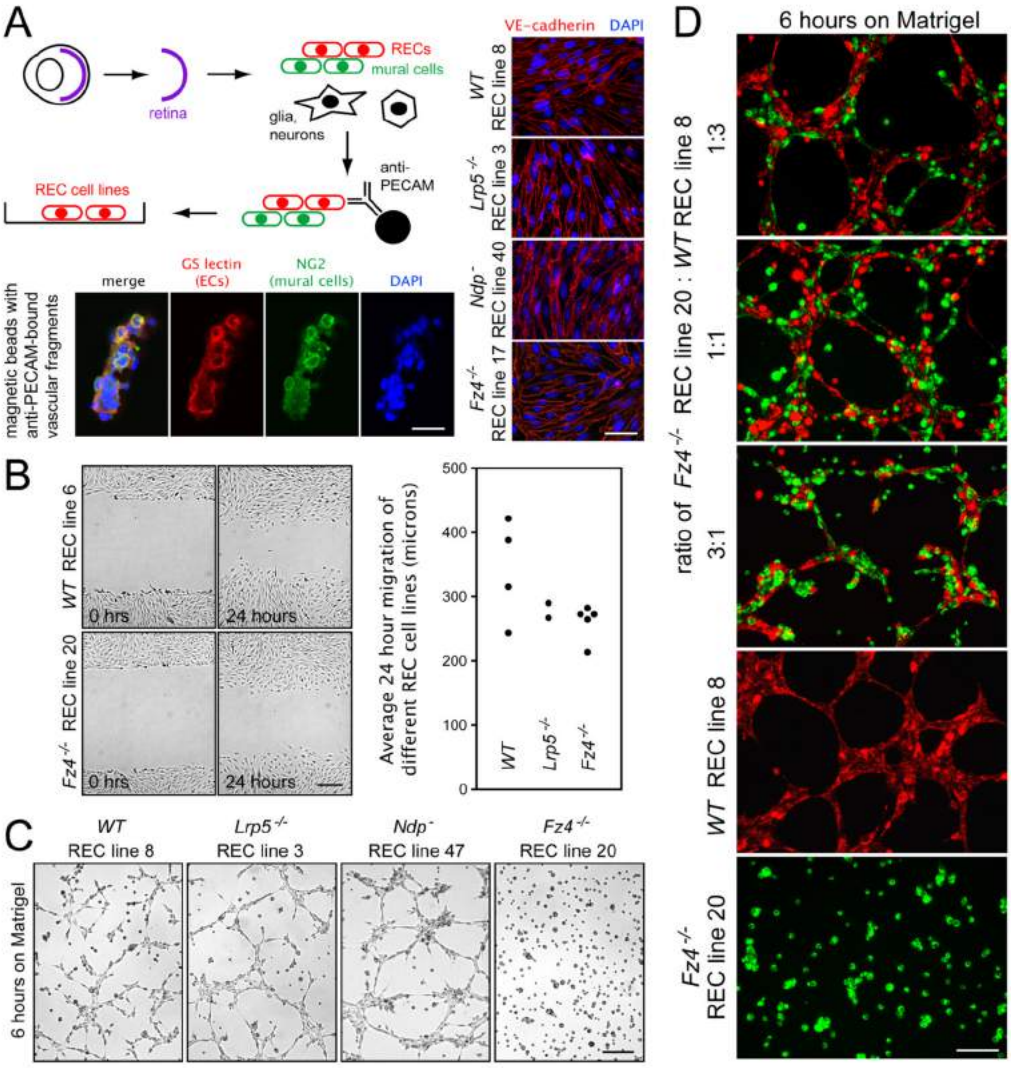

Figure 6.

Fz4$^{-/-}$ REC lines exhibit defects in the formation of capillary-like structures

(A) Diagram of immuno-affinity purification of vascular fragments (upper), and immunohistochemical characterization of isolated fragments (lower; scale bar 20 um) and cloned REC lines (right; scale bar, 50 um).

(B) Scratch-induced motility on gelatin-coated dishes. Left, phase contrast images zero and 24 hours after the scratch; right, quantification of cell motility. Scale bar, 200 um.

(C) WT, *Lrp5*$^{-/-}$, and *Ndp*$^{-}$ REC lines form capillary-like structures six hours after plating on Matrigel; *Fz4*$^{-/-}$ REC lines do not. Scale bar, 200 um.

(D) Matrigel cultures of diI-labeled WT and diO-labeled *Fz4*$^{-/-}$ RECs, mixed immediately before plating at the indicated ratios. Bottom, Matrigel cultures of the pure RECs. Scale bar, 100 um.

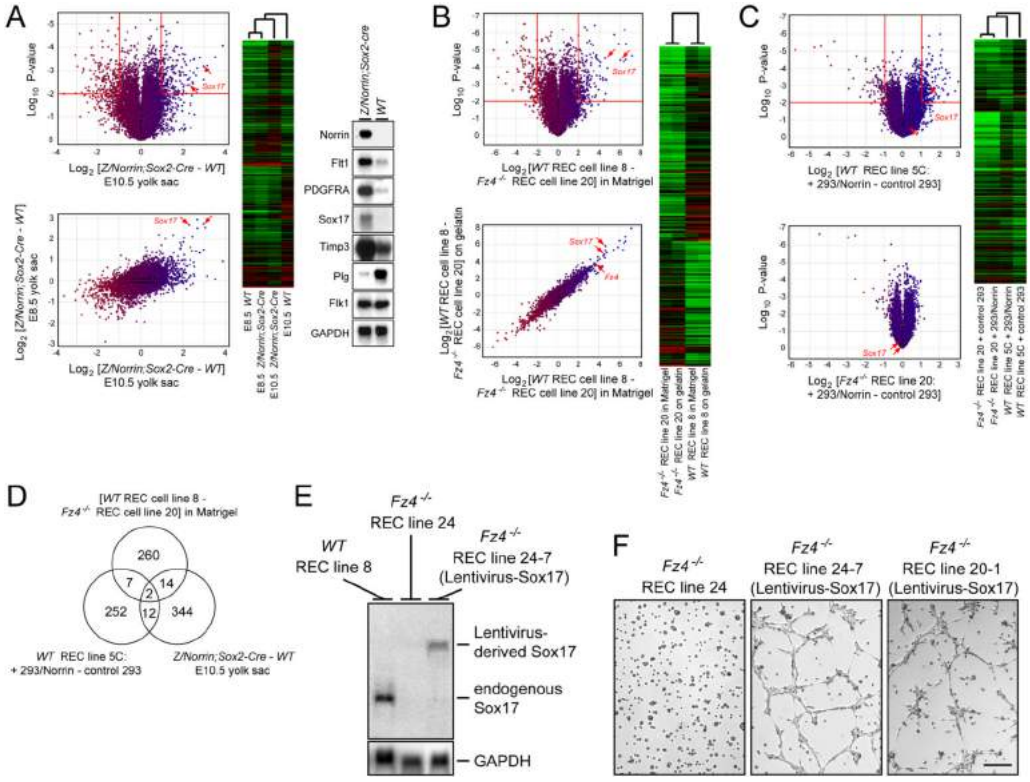

Figure 7.

Sox17 plays a critical role in the Norrin/Fz4/Lrp-dependent transcriptional program in ECs

(A) Norrin-induced changes in transcript abundances in WT vs. *Z/Norrin;Sox2-Cre* yolk sacs at E8.5 and E10.5. The heat map shows differences greater than 2-fold with a P-value <0.01 in the E10.5 WT vs. *Z/Norrin;Sox2-Cre* yolk sac comparison (red borders in upper plot). RNA blot hybridization of selected transcripts in E10.5 WT and *Z/Norrin;Sox2-Cre* yolk sacs confirms increased abundances of *Norrin*, *Flt1*, *PDGFRA*, *Sox17*, and *Timp3* transcripts, decreased abundances of *Plasminogen* (*Plg*) transcripts, and unaltered abundance of *Flk1* and *GAPDH* transcripts. Micro-array data in this Figure are averages of three independent experiments.

(B) Transcripts differences between WT and $Fz4^{-/-}$ REC lines (upper plot) are largely unaffected by growth on Matrigel vs. gelatin (lower plot). The heat map shows differences greater than 4-fold with a P-value <0.01 in WT vs. $Fz4^{-/-}$ REC lines (red borders in upper plot).

(C) Norrin-induced changes in transcript abundance in WT (upper plot) but not $Fz4^{-/-}$ (lower plot) REC lines. The heat map shows differences greater than 2-fold with a P-value <0.01 when WT RECs were co-cultured with 293/Norrin vs. control 293 cells (red borders in upper plot).

(D) Venn diagram indicating the overlap among transcripts delimited by the red borders in panels A–C.

(E) Sox17 transcripts are undetectable by RNA blotting in $Fz4^{-/-}$ RECs (center), but are present in $Fz4^{-/-}$ RECs following lentiviral transduction of Sox17 (right) at levels similar to those of WT RECs (left). The image is from one exposure of an RNA blot; for clarity, several lanes between lanes 2 and 3 have been removed.

(F) Lentivirus transduction of Sox17 rescues the ability of $Fz4^{-/-}$ RECs to form capillary-like structures in Matrigel. Results are shown for two independent $Fz4^{-/-}$ REC lines; the defective Matrigel behavior of the parental $Fz4^{-/-}$ REC line 20 is shown in Figure 6C.